

Formation of MFe_2O_4 ($M = Co, Ni$ and Mn) Films from MO / Fe_2O_3 Multilayers

Sayeduzzaman Syed^{1,2}, Daisuke Kubota¹, Y. Hosokawa¹, Ryoichi Nakatani¹

Division of Materials and Manufacturing Science, Graduate School of Engineering, Osaka University,

2-1 Yamadaoka, Suita, Osaka, Japan¹

Dept of Applied Physics, Electronics and Communication Engineering, Islamic University, Kushtia, Bangladesh²

Abstract: We have investigated the saturation magnetization and structure of MFe_2O_4 ($M = Co, Ni$ and Mn) films prepared by annealing process of MO (1 nm) / Fe_2O_3 (1 nm) multilayers. The highest saturation magnetization M_s of 330 G and spinel structure are obtained in insulating $CoFe_2O_4$ films after annealing at 773 K. In the case of our semi-conducting $NiFe_2O_4$ films, the highest saturation magnetization M_s of 167 G and iron segregated spinel structure are observed after annealing at 823 K. The highest saturation magnetization M_s of 198 G and spinel structure are found in $MnFe_2O_4$ films after annealing at 873 K. The spinel MFe_2O_4 films obtained by annealing are become the promising candidate materials for the research area of spintronics.

Keywords: annealing, spin polarization, saturation magnetization, spinel structure, half-metal and spin filter.

I. INTRODUCTION

Spintronic research deals with the spin direction of electron; as a result one can control the direction of spin of electron by magnetic fields and flow of electrons [1]. The spin polarization is of fundamental importance for the use of materials in spintronics applications. The spin polarization also determines the manipulation of magnetization itself and thus the realization of spin based logic circuits [2-3]. Spin transport through a device defines the current spin polarization, $P_1 = (i_{up, \alpha} - i_{down, \alpha}) / (i_{up, \alpha} + i_{down, \alpha})$; where $\alpha = d, sp$ orbit of the device materials [4]. One of the successful approaches is to manipulate the spin polarization through tunnelling probability by using a ferromagnetic insulator known as spin filter [5]. Some classical techniques to determine the spin polarization P of a material are spin-polarized photoemission, Meservey-Tedrow technique, Andreev reflection using superconducting contact [6-8]. An introduction of weakly polarized states at the Fermi level can also be realized in the materials itself by chemical bonding. These materials are called half-metals [9]. In contrast to the spin polarization, optical pump-probe experiments can determine the demagnetization time τ_m , which is related to the half-metallicity of the material [10]. The classification of different half-metals due to their transport characteristics was given by Coey et al [11]. The half-Heusler alloys, full-Heusler alloys and oxides are well known as highly (100%) spin-polarized materials [12-15]. Magnetic oxides are also the candidates for half-metals because of their high spin polarizations and high Curie temperatures [16]. The MFe_2O_4 ($M = Co, Ni$ and Mn) magnetic oxide films have been attracted much attention recently as the candidate materials for the research area of spintronics [17-19]. Several films preparation methods

have been introduced including sol-gel, sputtering, pulsed laser deposition (PLD), spin spray, chemical vapor deposition and molecular beam epitaxy [20-24]. Many research groups are investigating how to improve magnetic properties by controlling the structure or doping with different elements [25]. In this study, we will discuss the experimental results of MFe_2O_4 ($M = Co, Ni$ and Mn) films obtain from MO / Fe_2O_3 multilayers by annealing.

II. EXPERIMENTAL PROCEDURE

The 50-nm-thick $[MO (1 \text{ nm}) / Fe_2O_3 (1 \text{ nm})]_{25}$ ($M = Co, Ni$ and Mn) multilayers were fabricated at room temperature (RT) by ion beam sputtering (IBS) from MO and Fe_2O_3 targets on thermally-oxidized $Si(100)$ substrates. All multilayers were covered with 3-nm-thick SiO_2 layer as a capping layer in order to prevent oxidation. The base pressure of the apparatus was better than 1.0×10^{-4} Pa and the Ar pressure during sputtering was 0.002 Pa. The acceleration voltage of the ion gun was 600 V with the ion current of 60 mA. The deposition rates of $[MO / Fe_2O_3]$ multilayers and SiO_2 layers were 0.11 nm / sec and 0.12 nm / sec respectively. The thickness of MFe_2O_4 films was fixed at 50 nm. In order to obtain MFe_2O_4 films, the as-deposited multilayers were annealed at various temperatures (T_a) up to 823 K and carefully observed the magnetic properties and structure with T_a for the spinel structure formation of the films. The magnetization curves of the films were measured using a vibrating sample magnetometer at room temperature with the applied magnetic field of 10 kOe parallel to the films plane. The structures of the MFe_2O_4 films were determined by an X-ray diffractometer (XRD) with $Cu-K\alpha$ radiations.

III.RESULTS AND DISCUSSION

Fig.1. shows the change of saturation magnetization M_s of $CoFe_2O_4$ films with annealing temperatures T_a . The saturation magnetization M_s of $CoFe_2O_4$ films enhances from room temperature to annealing temperature up to 773 K and reduces in the films annealed at 823 K. The $CoFe_2O_4$ films annealed at 773 K shows the highest saturation magnetization M_s of 330 G. This changing behavior of magnetic properties is due to the structural change in $CoFe_2O_4$ films with annealing [26].

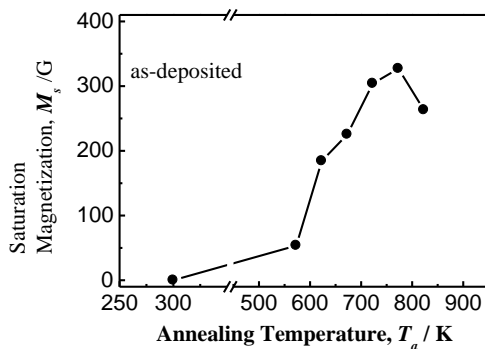


Fig.1. Change of saturation magnetization M_s of 50-nm-thick $CoFe_2O_4$ films as a function of annealing temperatures T_a

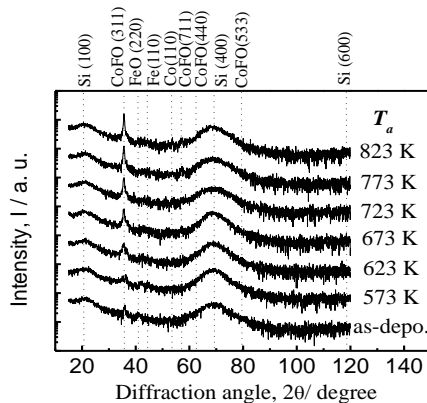


Fig.2. High angle XRD profile of the 50-nm-thick $CoFe_2O_4$ films annealed at various temperatures T_a

In order to observe the changes in $CoFe_2O_4$ films with annealing temperature T_a , we have performed XRD experiments. Fig.2. shows the XRD profiles of $CoFe_2O_4$ films before and after annealing at various temperatures T_a . The peak of bulk $CoFe_2O_4$ films (311), (711), (440), (533) and peak of bulk Fe (110) and Co (111) are shown by the broken line on XRD profile. Bulk peak of FeO (220) is also shown by the broken line on XRD profiles. Since the structure of Fe_3O_4 and $CoFe_2O_4$ films are similar spinel structures, therefore, the peaks of the Fe_3O_4 and

$CoFe_2O_4$ films are considered at the same position on the profile. Furthermore, peaks of Si (100), Si (400) and Si (600) originated from the thermally oxidized substrates are also shown by the broken line but the Si peaks of thermally-oxidized Si substrate are in amorphous condition so that the determination of Si and SiO_2 should be difficult. The peak at $2\theta = 35.8^\circ$ can be considered as the main peak of $CoFe_2O_4$ (311), similar to the main peak Fe_3O_4 spinel structure. The strength of this peak increases with annealing temperature up to 823 K. This means that the grain size of $CoFe_2O_4$ films also increases with annealing temperatures. A broad peak of FeO (220) appear at $2\theta = 35.8^\circ$ up to the annealing temperature of 723 K.

In the case of annealing above 723 K the diffracted peaks were found at $2\theta = 57^\circ, 62.5^\circ, 73.5^\circ$ on the XRD profile. These peak are the diffracted peak of $CoFe_2O_4$ (711), (440), (533) therefore, the spinel $CoFe_2O_4$ films is produced by annealing at 773 K. Again, in the case of annealing temperature 773 K, the main peaks of Fe (110) and Co (111) do not appear at $2\theta = 44.6^\circ$ and $2\theta = 53.6^\circ$ on the XRD profile, which determine the Fe particles and Co particles are not segregated in $CoFe_2O_4$ films. Furthermore, in the case of annealing of 823 K the appearance of two different peak at $2\theta = 47.6^\circ$ and $2\theta = 53.5^\circ$ indicate about the diffusion of oxygen atom from the multilayers during annealing, which may create defect in spinel structures. Another point view of crystal structure, the $CoFe_2O_4$ films obtain the attribute of spinel structure after annealing at 773 K.

The resistivity of the $CoFe_2O_4$ films has been observed in the range of $1 \times 10^{10} \Omega.cm$ to $1 \times 10^{10} \Omega.cm$ for all T_a , while the resistivity of metal is in the order of $10^{-4} \Omega.cm$ and the resistivity of semiconductor is in $10^{-3} \Omega.cm$ to $10^7 \Omega.cm$ [27]. Therefore, the resistivity of $CoFe_2O_4$ films is 10^3 times higher in the insulating range and thus the $CoFe_2O_4$ films can be determined as magnetic insulator.

Fig.3. shows the change of saturation magnetization M_s of $NiFe_2O_4$ films with annealing temperatures T_a . The saturation magnetization M_s increases from room temperature to the annealing temperature up to 823 K. The maximum saturation magnetization, M_s of 218 G is obtained after annealing at 823 K, however, as-deposited $NiFe_2O_4$ films does not show any magnetization. The reported bulk value of saturation magnetization of $NiFe_2O_4$ ferrite is 300 G [28].

But our experimental result is much lower than that of the reported value. However, the properties of bulk materials and thin layers are also different. There are such examples in materials having spinel structure for obtaining different saturation magnetization between the bulk and thin films [28-29]. Again, since Fe is ferromagnetic particle, therefore, Fe particles have contribution to the enhancement of saturation magnetization in $NiFe_2O_4$ with annealing temperature.

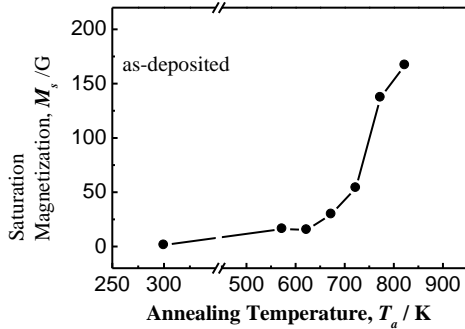


Fig.3. Change of saturation magnetization M_s of 50-nm-thick $NiFe_2O_4$ films as a function of annealing temperatures T_a

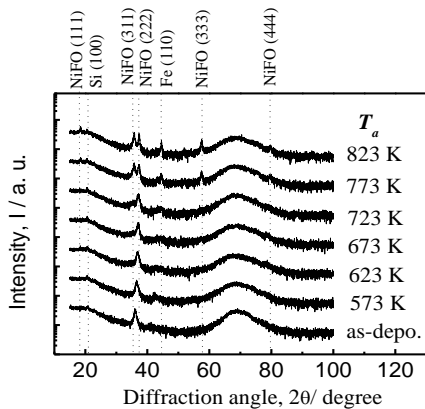


Fig.4. High angle XRD profile of the 50-nm-thick $NiFe_2O_4$ films annealed at various temperatures T_a

Due to the above reason, the experimental results differ from that of the bulk value of $NiFe_2O_4$. Consequently, the experimental results of the fabricated $NiFe_2O_4$ cannot be comparable to the bulk value.

Especially, in the case of multilayers, the saturation magnetization may be obtain near to the bulk value of $NiFe_2O_4$ films after annealing above 823 K, however, the similar saturation magnetization does not mean that the perfect $NiFe_2O_4$ films can be produced above $T_a = 823$ K. Rather, Fe particle dominate the $NiFe_2O_4$ films above 823 K, which results lower resistivity in $NiFe_2O_4$ films. The measured resistivity of the $NiFe_2O_4$ films for all T_a is observed in the range of 0.5 Ω .cm to 1.2 Ω .cm and thus the $NiFe_2O_4$ films can be determined as magnetic semiconductor.

The structural changes of $NiFe_2O_4$ films with annealing temperature T_a is shown in Fig.4. The peak of bulk $NiFe_2O_4$ films (111) (311), (222), (333), (444) and peak of bulk Fe (110) are shown by the broken line on XRD profile. Furthermore, Si substrate peaks are not shown on the XRD profile because of the amorphous condition of the thermally oxidized Si substrates. The peaks at $2\theta = 35.8^\circ$ and 37.8° can be considered as the main peak of

$NiFe_2O_4$ (311) and (222), similar to the main peak $CoFe_2O_4$ spinel structure. The strength of this peak increases with annealing temperature up to 823 K. This means that the grain size of $NiFe_2O_4$ films also increases with annealing temperatures. In the case of annealing above 723 K the diffracted peaks were found at $2\theta = 57^\circ, 80^\circ$ on the XRD profile. These peak are the diffracted peak of $NiFe_2O_4$ (333) and (444) therefore, the $NiFe_2O_4$ films is produced with spinel structure by annealing at 773 K. Again, in the case of annealing temperature above 773 K, the main peaks of Fe (110) appears at $2\theta = 44.6^\circ$ on the XRD profile, which determine the Fe particles are segregated in $NiFe_2O_4$ films. From the point view of crystal structure, the $NiFe_2O_4$ films attain iron segregated spinel structure after annealing above 773 K.

Again, Fig.5. Show the change of saturation magnetization, M_s of $MnFe_2O_4$ films with annealing temperature up to 873 K. The saturation magnetization of the $MnFe_2O_4$ films increases gradually from the as-deposited value to annealing temperature $T_a = 823$ K and rapidly increases for the films annealed up to 873 K. The maximum saturation magnetization, M_s of 198 G is obtained from the $MnFe_2O_4$ films annealed at 823 K.

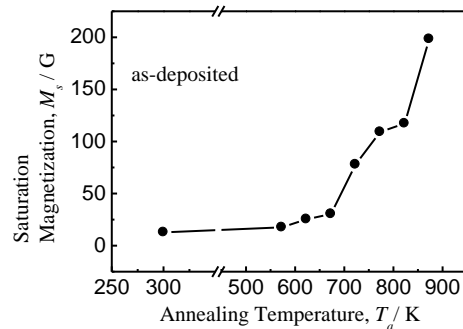


Fig.5. Change of saturation magnetization M_s of 50-nm-thick $MnFe_2O_4$ films as a function of annealing temperatures T_a

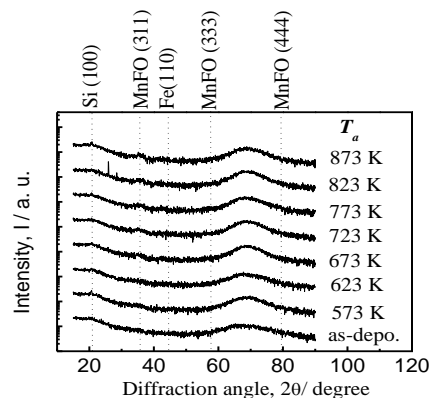


Fig.6. High angle XRD profile of the 50-nm-thick $MnFe_2O_4$ films annealed at various temperatures T_a

The structural changes of MnFe_2O_4 films as a function of annealing temperature T_a is also shown on the XRD profile in Fig.6. The crystal structure of the MnFe_2O_4 films annealed up to 723 K shows only the amorphous conditions of the film structures. The main peak of spinel MnFe_2O_4 (311) is observed on the XRD profiles of MnFe_2O_4 films annealed above 773 K. This spinel MnFe_2O_4 (311) peak strength increases up to annealing temperature 873 K. Therefore, The MnFe_2O_4 films annealed at 873 K show the highest saturation magnetization, M_s of 198 G and spinel crystal structure.

IV. CONCLUSION

We have successfully obtain the spinel MFe_2O_4 ($M = \text{Co}$, Ni and Mn) films from MO (1 nm) / Fe_2O_3 (1 nm) multilayers by annealing. The insulating CoFe_2O_4 films show highest saturation magnetization, M_s of 330 G and spinel structure after annealing at 773 K. The semi-conducting NiFe_2O_4 films show the highest saturation M_s of 167 G and Fe segregated spinel structure after annealing at 823 K. The highest saturation magnetization, M_s of 198 G and spinel structure are observed in the MnFe_2O_4 films after annealing at 873 K. Our experimental results suggest that the spinel MFe_2O_4 films can be considered as the half-metallic oxide materials or half-metals. The properties of MFe_2O_4 films obtain from multilayers are the promising properties for spintronic device materials.

ACKNOWLEDGMENT

The authors would like to thank to the Ministry of Education, Culture, Sports, Science and Technology (MEXT), Japan for the financial support (Scholarship) of this research work.

REFERENCES

- [1] Spin Electronics, edited by M. Ziese and M. J. Thornton, Lecture notes in Physics Vol. 569 (Springer, Berlin 2001)
- [2] S. I. Kiselev, et al, Nature 425, (2003) 380-383
- [3] G. Reiss, & Meyners, J. Phys. Condens. Matter, 19 (2007) 165220-165242
- [4] M. B. Stearns, J. Mang. Magn Matter. 5 (1977) 167-171
- [5] T. Nagahama, T. S. Santos and J. S. Moodera, Phys. Rev. Lett. 99 (2007) 016602
- [6] E. Vescovo et al. Phys. Rev. B 56 (1997) R11403-R11406
- [7] R. Meservey, P. M. Tedrow, Physics Reports 238 (1994) 173-243
- [8] R. J. Soulen Jr. et al. Science. 282 (1998) 85-88
- [9] R. A. de Groot, F. M. Muller, P.G. Van Engen & K. H. J. Buschow, Phys. Rev. Lett. 50 (1983) 2024-2027
- [10] G. M. Muller et al, Nature Materials. 08 (2009) 56-61
- [11] M. Venkatesan, in Handbook of Magnetism and Advanced Magnetic Materials Vol. 4 Novel Materials (2007)
- [12] C. T. Tanaka, J. Noak and J. S. Moodera, J. Appl. Phys. 81 (1997) 5515-5517
- [13] Ishida, S. Fujii, S. Kashiwagi and S. Asano, J. Phys. Soc. Jpn. 64 (1995) 2152-2157
- [14] M. Y. Sakuraba, J. Nakata, M. Oogane, H. Kubota, Y. Ando, A. Sakuma and T. Miyazaki, Jpn. J. Appl. Phys. 44 (2005) L1100-L1102
- [15] R.A. de Groot and K.H.J. Buschow, J. Magn. Magn. Matter. 54-57 (1986) 1377-1380
- [16] Y. Suzuki, R. B. van Dover, E. M. Gyorgy, Julia M. Phillips, V. Korenivski, D. J. Werder, C. H. Chen, R. J. Cava, J. J. Krajewski, and W. F. Peck, Jr. K. B. Do, Appl. Phys. Lett. 68 (1996) 714
- [17] B. B. Nelson-Cheeseman, R. V. Chopdekar, J. S. Bettinger, E. Arenholz, and Y. Suzuki, J. Appl. Phys. 103 (2008) 07B524
- [18] Y. Kitamoto S. Kantake, S. Shirasaki, F. Abe, and M. Naoe, J. Appl. Phys. 85 (1999) 4708
- [19] W. F. J. Fontijn, P.J. vander Zagg, L.F. Feiner, R. Metselaar, and M. A. C. Devellers, J. Appl. Phys. 85 (1999) 5100
- [20] J. G. Lee and J. Y. Park, J. Appl. Phys. 84 (1998) 2801
- [21] J. Ding et al., Appl. Phys. Lett., 77 (2000) 3621
- [22] Y. C. Wang et al, Appl. Phys. Lett., 84 (2004) 2596
- [23] A. G. Fitzgerald and T.G. May, Thin Solid Films, 35 (1976) 201
- [24] S. A. Chambers et al., J. Magn. Magn. Matter. 246 (2004) 124
- [25] Y. Suzuki, R.B. van Dover, E.M. Gyorgy, Julia M. Phillips, V. Korenivski, D. J. Werder, C. H. Chen, R. J. Cava, J. J. Krajewski, W. F. Peck, Jr. and K. B. Do, Appl. Phys. Lett. 68 (1996) 714
- [26] S. Syed, Y. Endo, T. Sato, Y. Kawamura and R. Nakatani, Materials Transactions, Vol 49, No.1(2008) pp. 175 to 178
- [27] S. Chikazumi, Physics of the ferromagnetism, Oxford science publication
- [28] U. Luders, M. Bibes, K. Bouzehouane, E. Jacquet, J. P. Contour, S. Fusil, J. Fontcubetra, A. Barthelemy, and A. Fert, Appl. Phys. Lett. 88 (2006) 082505
- [29] A. V. Romas, J. B. Moussy, M. J. Guittet, M. Gautier Soyer, C. Gatel, P. Bayle Guillemaud, B. Warot Fonrose, and E. Snoeck, Phys. Rev. B 75 (2007) 22442